Improved Antenna Phase Center Offsets for BDS-2 IGSO/MEO Satellites Based on MGEX Long-Term Observations

LINA HE[1], PING ZENG[1], HAIRUI ZHOU[2], (Member, IEEE), AND YUANLAN WEN[1]

[1]School of Earth Sciences and Engineering, Hohai University, Nanjing 211100, China
[2]28th Institute, China Electronics Technology Group Corporation, Nanjing 210007, China

Corresponding authors: Lina He (hlnyh@hhu.edu.cn) and Yuanlan Wen (wenyuanlan@hhu.edu.cn)

ABSTRACT For the purpose of further improving the solution accuracies of the orbital and geodetic parameters for BDS (BeiDou Navigation Satellite System) precise applications, this paper focuses on the enhancements of antenna phase center offsets (PCOs) for BDS-2 IGSOs (Inclined Geosynchronous Satellite Orbits) and MEOs (Medium Earth Orbits) through processing observations from a global tracking network. The daily estimated horizontal and vertical PCO time series of nearly three years from DOY (Day of Year) 001 in 2018 to DOY 180 in 2020 are obtained using the PANDA (Position And Navigation Data Analysis) software. The long-term PCO time series have seasonal variations and systematic effects along with the elevation angle of the Sun with respect to the orbital plane. Then, type-specific x-offsets and y-offsets of IGSOs and MEOs are comprehensively available considering the good consistency for the same satellite type. And a set of satellite-specific vertical offsets are recommended to BDS-2 IGSOs and MEOs since the low coherence of these satellites with the same type. Validation experiments are carried out for comparison between the original MGEX (Multi-GNSS Experiment) PCOs and the newly improved values (iMGEX PCOs for short), including the Precise Orbit Determination (POD) and Precise Point Positioning (PPP). Based on the orbital overlap analysis, the qualities of BDS-2 orbits show great enhancements in the along-track, cross-track and radial components, when the iMGEX PCOs are employed. Results of the independent assessment using SLR (Satellite Laser Ranging) also indicate the improvements on the radial component for C08, C10 and C11 satellites, and most of the orbit RMSs (Root Mean Squares) of iMGEX results decreased by 40.5% on average compared with the MGEX values. Additionally, the experimental station coordinates by static PPP achieve improvements at the rate of 27.1%, 32.6% and 28.4% in the east, north, and up component, respectively, in which more than a half stations realize sub-centimeter positioning accuracy in the north component using the iMGEX PCOs.

INDEX TERMS BeiDou navigation satellite system, antenna phase center offset, precise orbit determination, precise point positioning.

I. INTRODUCTION

As a newly built constellation, BDS (BeiDou Navigation Satellite System) is distinct with other navigation satellite systems as its hybrid constellation, multiple frequencies and communication capabilities [1]. And the successful experience of GPS (Global Positioning System) is not always

The associate editor coordinating the review of this manuscript and approving it for publication was Halil Ersin Soken.

suitable for BDS. In order to realize high precision applications of BDS, numerous efforts are made to enhance the solution strategies, force models and error corrections for better orbit and clock products [2]. It is well known that precise orbit products for GNSS (Global Navigation Satellite System) satellites are related to their CoMs (Center of Masses), while the observations refer to the antenna phase centers [3]. The offsets between the CoMs and the antenna phase centers, called PCOs (Phase Center Offsets), are necessary to correct

for high precision applications [4]. However, it is difficult to measure PCO and its variations due to the fact that the antenna phase center is not a physical point but an electrical one varying time to time [5]. In early solutions, PCO corrections for both satellites and receivers are partly neglected for GNSS signals, since they are not officially available [6]. Hence, the PCOs of satellites are considered as one of the potential factors to further improve the accuracies of POD (Precise Orbit Determination) and PPP (Precise Point Positioning) solutions [7].

Generally, satellite PCO is provided by the manufactory according to satellite hardware construction or calibration before satellite launched. However, it is reported that only a few backbone types of satellites, e.g., GPS Block IIA, were calibrated for the absolute antenna phase center [8]. Meanwhile, the PCOs will be changing with the unstable space environments and the varying satellite statuses. Based on these reasons, the IGS (International GNSS Service) intended to estimate PCOs and their variations for different GNSS satellites by processing the global tracking network datasets [9]. Schmid and Rothacher have already published the GPS PCOs [10], but they are the block-specific corrections, which are not sufficient as GPS satellites have unique PCO values with remarkable difference between each other [11]. Besides, long-term solutions are necessary to integrate the mean PCOs for the scale inconsistency reason [12]. Meanwhile, GLONASS (Global Navigation Satellite System) PCOs are also proposed base on more data 1.6 years observation datasets [13]. In parallel to GPS and GLONASS, continuous efforts are also made to the newly established navigation satellite systems, i.e., Galileo [14], BDS [15], QZSS (Japanese Quasi-Zenith Satellite System) [16] and IRNSS (Indian Regional Navigation Satellite System) [17]. In mid of 2015, IGS antenna files provide antenna parameters of these new constellations for the first time [18].

From the experiences of GPS and other systems, antenna parameters of the BDS satellites also can be achieved. Lou indicates that the manufacturer's nominal PCO is (634.00, −3.00, 1075.00) mm for x-, y- and z- offset, respectively, and it is adopted in the early BDS-2 precise orbit determination [19]. Meanwhile, the MGEX (Multi-GNSS Experiment) recommends PCO as (200.00, 0.00, 1100.00) mm, and are used by some analysis centers, such as GFZ (Deutsche GeoForschungsZentrum). From the GPS day 17994, WHU (Wuhan University) has updated the PCO values of BDS-2 IGSOs (Inclined Geosynchronous Orbits) and MEOs (Medium Earth Orbits) by processing global observation datasets from multiple tracking networks, i.e., MGEX, BETN (BeiDou Experimental Tracking Network) and iGMAS (International GNSS Monitoring and Assessment System) [20]. ESA/ESOC (European Space Agency/European Space Operations Centre) estimates PCOs for BDS-2 IGSOs and MEOs using more than one year observations, and the constellation-specific x-offset of about 550.00 mm, y-offset of 0.00 mm and satellite-specific z-offsets of about 2000.00 mm are obtained [21]. CHA

(Chang'an University) gives the PCOs of BDS-2 IGSOs and MEOs based on one year observation data and concludes their estimated PCOs are of higher accuracy compared with WHU and ESA/ESOC under their processing strategies [22]. Afterwards, PCO conventions of BDS-2 satellites are recommended by MGEX with (600.00, 0.00, 1100.00) mm until further notice [23]. In addition, IGS has collected and published the latest updated PCOs of BDS in the igs14_2056.atx, but just for block-specific values [24].

Although many efforts have given improved PCO values for BDS, however, these values change with operational status of each satellite and the complex space environments [25]. It is reported that different attitude models have been used for the newly launched IGSO satellite (C13) and another two BDS-2 MEOs (C06 and C14) according to the motion of an orbiting satellite [26]. Since the satellite PCO is related to the attitude model, the PCO value should be reestimated when a new attitude model is established. Meanwhile, the CoM of a satellite also changes because of the fuel consumption and components aging. Hence, the PCO of a satellite has to be determined and updated continuously [25]. Further, previous studies usually employ only one year's observations to calculate PCOs. Considering the period of the elevation angle of the Sun with respect to the orbital plane is a year for BDS satellites, the long-term observations will be better for improving the accuracy, reliability, and consistency of the PCO results [3]. More importantly, the latest PCOs of BDS satellites, which are available within igs14_2056.atx, are type-specific values for IGSOs and MEOs, and experiments validate that the more sophisticated PCOs lead to more precise POD and PPP results [25]. In this paper, improved PCOs for BDS-2 IGSOs and MEOs based on long-term observations are proposed, in which GEOs are excluded due to the weak ground station observation geometry [27]. Another thing to note is that the BDS-3 PCOs are not processed here but will be considered in the future as long as the enough observations are available.

The rest of the paper is organized as follows, in Section II, the PCO modeling is presented. Meanwhile, the processing strategies for antenna parameters of BDS-2 satellites are given in Section III. Then, the daily estimated PCO time series for BDS-2 satellites are obtained and analyzed, and the type-specific x-offsets and y-offsets, as well as satellite-specific z-offsets, are comprehensively generated with the weighted mean method in Section IV. Further, the performances of the improved PCO results are investigated based on the POD and PPP solutions in Section V. Finally, the conclusions are drawn in Section VI.

II. THE PCO MODELLING

As mentioned in Section I, the CoM is a reference point for describing the satellite motion, and GNSS observations always refer to the antenna phase center, which is neither a physical nor a stable point in space. The difference between the antenna phase center and the CoM is called PCO. As shown in Fig.1, the satellite body-fixed reference system is
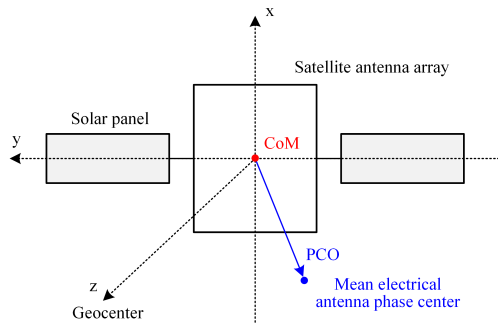
FIGURE 1. The satellite body-fixed reference system and the relationships between the CoM and antenna phase center.

usually employed for describing the PCO corrections. This reference system is related to the mechanical structure of a satellite permanently and the origin coincides with the CoM. The z-axis aligns with the boresight of transmitting antenna towards the geocenter ideally. The y-axis points along the rotation axis of the solar panels. And the x-axis points to the Sun positively to complete the right hand system [28]. According to this definition, z-offset is in the antenna bore-sight direction, and called vertical PCO, while x-offset and y-offset are called horizontal PCOs.

Theoretically, the satellite PCOs should be added into the observation equations and estimated during the sophisticated orbit determination processing. Firstly, the satellite position can be obtained by a second order satellite motion differential equation described as follows,

$$\ddot{\mathbf{r}} = -\frac{GM}{r^3}\mathbf{r} + \mathbf{a}_{ns} + \mathbf{a}_{tb} + \mathbf{a}_{tide} + \mathbf{a}_{rel} + \mathbf{a}_{srp} + \mathbf{a}_{erp} \quad (1)$$

where $\ddot{\mathbf{r}}$, $\mathbf{r}$ denote the acceleration and position vectors of a satellite. G is the gravitation constant and M is the mass of the Earth. $\mathbf{a}_{ns}$ is the gravitational potential of an aspherical body caused by the non-spherical shape and uneven mass distribution of the Earth. $\mathbf{a}_{tb}$ refers to the gravitational perturbation accelerations caused by main planets (the Sun, the Moon and other planets) except the Earth. $\mathbf{a}_{tide}$ represents the orbital perturbations of the Earth's solid and ocean tides. $\mathbf{a}_{rel}$ is the direct perturbation of the relativistic effects. $\mathbf{a}_{srp}$ stands for the perturbation accelerations resulting from the solar radiation pressure. $\mathbf{a}_{erp}$ represents the perturbation accelerations derived by the Earth radiation pressure [29].

Then, the rough position of a satellite can be improved by the tracking observations, and the observation equations can be expressed as follows,

$$\rho_{obs} = \rho_k^s + c \cdot \left(\delta t_k - \delta t^s\right) + \Delta\rho_{tro} + \Delta\rho_{ion} + \Delta\rho_{rel}$$
$$- \Delta\rho^{s,ant} + \Delta\rho_k^{ant} + \varepsilon_\rho \quad (2)$$

$$\phi_{obs} = \rho_k^s + c \cdot \left(\delta t_k - \delta t^s\right) + \Delta\rho_{tro} - \Delta\rho_{ion} + \Delta\rho_{rel}$$
$$- \Delta\rho^{s,ant} + \Delta\rho_k^{ant} + \lambda N^s + \varepsilon_\phi \quad (3)$$

where ρ_{obs} and ϕ_{obs} are the pseudo-range and carrier phase observations of receiver k to the instantaneous antenna phase center of satellite s. c is the light speed in the vacuum. δt_k and

δt^s are the clock offsets of receiver k and satellite s. $\Delta\rho_{tro}$ and $\Delta\rho_{ion}$ are the tropospheric and ionospheric delays. $\Delta\rho_{rel}$ is the relativistic effect correction. $\Delta\rho^{s,ant}$ and $\Delta\rho_k^{ant}$ are the antenna phase center corrections of satellite s and receiver k. λ is the wavelength of the carrier phase observation. N^s is the integer ambiguity. ε_ρ represents the unmodeled errors and pseudo-range observation noises, and ε_ϕ represents the unmodeled errors and carrier phase observation noises. ρ_k^s is the geometric distance between the mean phase center (MPC) of receiver k and satellite s.

As a part of the observation equations, the satellite PCOs in the inertial system can be expressed by Equation (4) and estimated by the least squares algorithm with the aid of Equation (1), (2) and (3). Supposing that the antenna phase center in the satellite body-fixed system is $\mathbf{x}_{pco}$, then the PCO in the inertia system ($\mathbf{x}^{s,ant}$) can be described as follows based on the satellite CoM.

$$\rho_k^s = \sqrt{\left\|\mathbf{x}^{s,ant} - \mathbf{x}_k^{ant}\right\|}$$
$$= \sqrt{\mathbf{x}^{s,CoM} + \mathbf{R}_{sbf \to cis} \cdot \mathbf{x}_{pco} - \mathbf{x}_k^{ant}} \quad (4)$$

where $\mathbf{x}^{s,ant}$ and $\mathbf{x}_k^{ant}$ are the vectors of the satellite and receiver PCOs in the inertial system, $\mathbf{x}^{s,CoM}$ is the vector of the satellite CoM in the inertial system, $\mathbf{R}_{sbf \to cis}$ is the rotation matrix from the satellite body-fixed system to the inertial system [28].

III. PROCESSING STRATEGY

The PCOs of BDS satellites can be determined together with other geodetic parameters, i.e., satellite orbit and clock. It is noting that the BDS-3 constellation has been successfully completed in Jun. 2020, but the number of the tracking stations for BDS-3 signals is not as many as required, so the accuracies of orbit and clock products are low in the early stage of the BDS-3 constellation due to the fact the observation dataset is not enough, and it is insufficient to ensure the accuracy of the PCO calculation. Therefore, the PCOs of BDS-3 satellites will be considered in our future work. Additionally, it is noting that the geometries of GEOs are special compared to IGSOs and MEOs. The locations of GEOs are relatively static seen from the tracking stations with little elevation angle changing [30]. Besides, GEOs employs the orbit-normal attitude mode all the time, in which the x-axis is along with satellite velocity direction and the y-axis is aligned perpendicular to the orbit plane [31]. Therefore, the orbit and clock products of GEOs are not as precise as IGSOs and MEOs, which prevent the stability and accuracy of their PCO estimations [27]. Based on these reasons, the PCOs of BDS-2 IGSOs and MEOs are focused in this paper.

MGEX recommended values (580.00, 0.00, 3500.00) mm for IGSOs and (580.00, 0.00, 2120.00) mm for MEOs are input as prior information for improving PCOs of BDS-2 satellites [24]. The ionosphere-free linear combination observations of GPS L1/L2 and BDS-2 B1/B2 are taken as input data to eliminate the first order ionosphere refraction effects. Accordingly, the estimations of PCOs refer to the com-

TABLE 1. Main processing strategies and parameters.

Item	Description
Number of stations	Approximately 130 stations including more than 50% GPS/BDS combined stations
Number of satellites	GPS: 31; BDS: 9 (6IGSOs, 3MEOs)
Time span	DOY 001 in 2018 to DOY 180 in 2020
Observations	Undifferenced ionosphere-free code and phase combination of dual-frequency (GPS:L1/L2; BDS:B1/B2)
Cut-off elevation	7 deg
Sample interval	300s
Weighting	elevation (E) dependent: 1.0 for E > 30°, 2sin(E) for E ≤ 30°
Ambiguity fixing	Ambiguity fixed for IGSOs and MEOs [33]
Inter-system biases	Estimated as constant
Orbits	Daily orbit arc ECOM without a priori model [34]
Station coordinates	Fixed (or tightly constrained)
Terrestrial frame	ITRF2014
Troposphere refraction	GMF [35], a priori model [36]
Earth gravity	EIGEN-6C 12×12
Tide displacement	IERS conventions 2010
Relativity effect	IERS conventions 2010
Satellite Antenna PCO	GPS satellite fixed to igs14_2056.atx; daily estimated for PCO of BDS satellite
Satellite Antenna PCV	Fixed to igs14_2056.atx
Receiver PCO/PCV	Fixed to igs14_2056.atx

bined frequency of B1/B2, not for B1 or B2 separately. Due to the fact that there are no official PCO calibrations for BDS-2 receivers, most efforts employ the values of the GPS receivers [32]. Similarly, in this paper, the IGS recommendations for the GPS receivers from igs14_2056.atx are applied for the BDS-2 receivers. Meanwhile, the estimations of BDS-2 PCOs are highly correlated with the terrestrial reference frame, and require sufficient constraints on scale [13]. Therefore, the combined GPS/BDS strategy is used for the PCO estimation in the daily POD processing to provide a stronger scale. Here, the main processing strategies and parameters are listed in Table 1.

In order to obtain a better geometry and more stable terrestrial scale, an optimal selection for the stations distribution is applied. Firstly, the ground tracking stations are distributed evenly in the world wide. Secondly, more than a half of stations provide high quality signals of BDS-2. Therefore, a network comprising approximately 130 stations is used in which above 65 stations have BDS-2 observations. The distribution of these stations is plotted in Fig.2, and it can be seen that there are two intensive areas of BDS-2 tracking stations, one is in Asia-Pacific, and it allows the constellation coverage to remain at nominal performance levels. And another is in Europe, mainly due to the fact that the scientific facilities in Europe are perfect, and the observations with good quality are available. Then, nearly three years of daily code and phase observations from MGEX network are collected in this study from Jan. 2018 to Jun. 2020, because the data qualities of BDS-2 from MGEX stations are more consistent and stable after the year of 2016 [17].

Additionally, the attitude models of BDS-2 are different with other navigation satellite systems. BDS-2 IGSOs and MEOs employ either yaw-steering or orbit-normal models for different situations depending on the elevation angel β of the Sun above the satellite orbit plane. The yaw-steering model is applied outside of the eclipse periods. When the β angle is
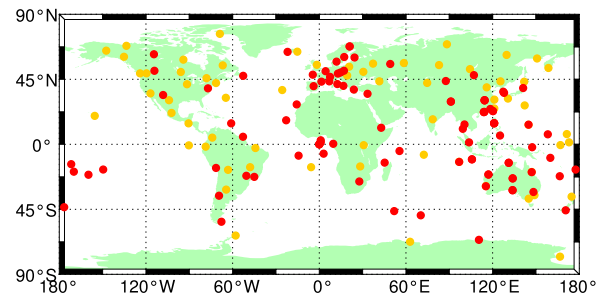
FIGURE 2. An optimal selection for the stations distribution (GPS stations are denoted in yellow, and GPS/BDS stations are denoted in red).

close to zero ($-4°$ to $4°$), the attitude model will be changed from yaw-steering to orbit-normal. Furthermore, C06, C13 and C14 employ a former attitude model at their early times and the new attitude model after 2017059, 2016089, and 2016300 respectively [37]. The PCO estimations will be reliable only if the attitude model is used properly during POD. Therefore, the attitude model should be considered carefully when determining PCOs.

Further, the processing diagram for the daily estimated PCOs in the PANDA (Position And Navigation Data Analysis) software are given in Fig.3. First of all, data preprocessing is carried out station by station for quality control. The main purpose is to explore cycle slips and flag ambiguities, inconsistencies and missing information. Then, based on initial conditions obtained from broadcast ephemeris, an integrated orbit is generated according to force models, e.g., non-spherical perturbation, tidal perturbation (solid, ocean and pole), the third-body perturbation, the solar radiation pressure and so on. In the next step, least squares estimation is performed to estimate the geodetic parameters including satellite PCO values. Specific to the PCO solution, firstly, in the parameter initialization, PCOs are set up to the MGEX values obtained from igs14_2056.atx file, and added into
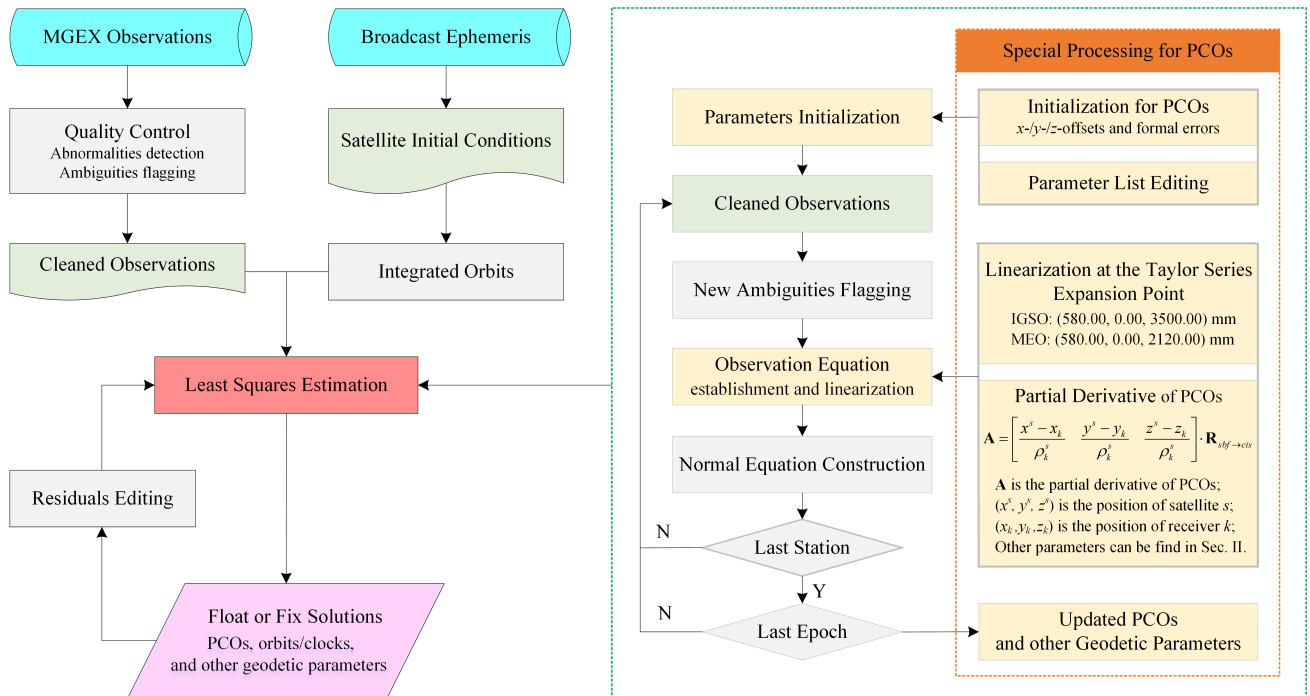
FIGURE 3. Precise orbit determination procedure for daily estimated PCOs.

the resolving parameter list. Then, observation equations are established and linearized by considering kinds of error corrections for each satellite. In this step, the partial derivative of the PCO variable can be solved by the Taylor series at the previous epoch as the linearization coefficient of the observation equations. Then, the normal equation in the least squares estimation can be obtained to update the estimated parameters based on post-fit residuals. Therefore, a float solution can be obtained with iteratively running until no cycle slip and outlier is found. Further, ambiguity fixing can be performed to obtain the fixed solution [33], in which satellite PCOs and other geodetic parameters can be updated as the final results.

IV. RESULTS AND ANALYSIS

Based on processing strategies described in Section III, the daily estimated PCOs are obtained using nearly three years MGEX observations. Firstly, the daily estimated PCO time series are presented and analyzed, including x-offsets, y-offsets and z-offsets. Secondly, the type-specific horizontal PCOs and satellite-specific vertical PCOs are derived by weighted mean method.

A. SPECIFIC CONSTRAINTS OF BDS-2 PCOs DURING ORBIT-NORMAL PHASES

The orbit-normal attitude mode used by BDS-2 satellite makes it challenging to estimate a reliable PCO during the deep eclipse season. This happens because the specific attitude mode (x-axis towards the velocity direction) adopted by BDS-2 satellites introduces strong correlations between the estimated PCOs and other parameters during
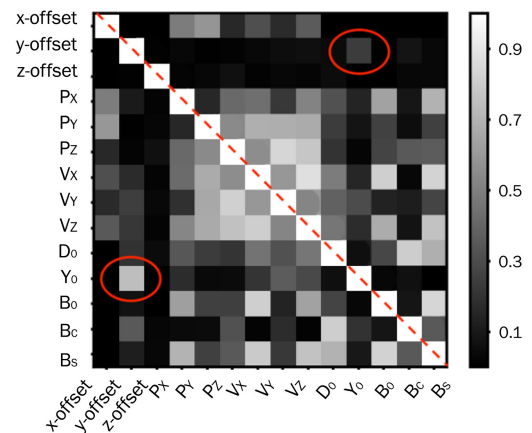

FIGURE 4. Correlation coefficients between PCOs (x-offset, y-offset and z-offset), orbital position (P_X, P_Y and P_Z), velocity (V_X, V_Y and V_Z) and ECOM parameters (three constants as D_0, Y_0 and B_0 and two periodic parameters B_c and B_s) at the initial epoch for C10 on DOY 010, 2018. The lower triangle section shows the correlation matrix with loose constraints, while the upper triangle one with tight constraint on y-offset.

POD processing, which in turn destabilizes the solution. Fig.4 gives an example of the correlation matrix between PCOs and orbital dynamic parameters during DOY 010 in 2018 when C10 is in the orbit-normal mode. The relationships between two parameters are described by the gray level of the matrix element. The lighter the color, the stronger the correlations.

It can be seen that y-offset is highly correlated (with coefficient up to 0.8) to the parameter Y_0 along y-axis in ECOM
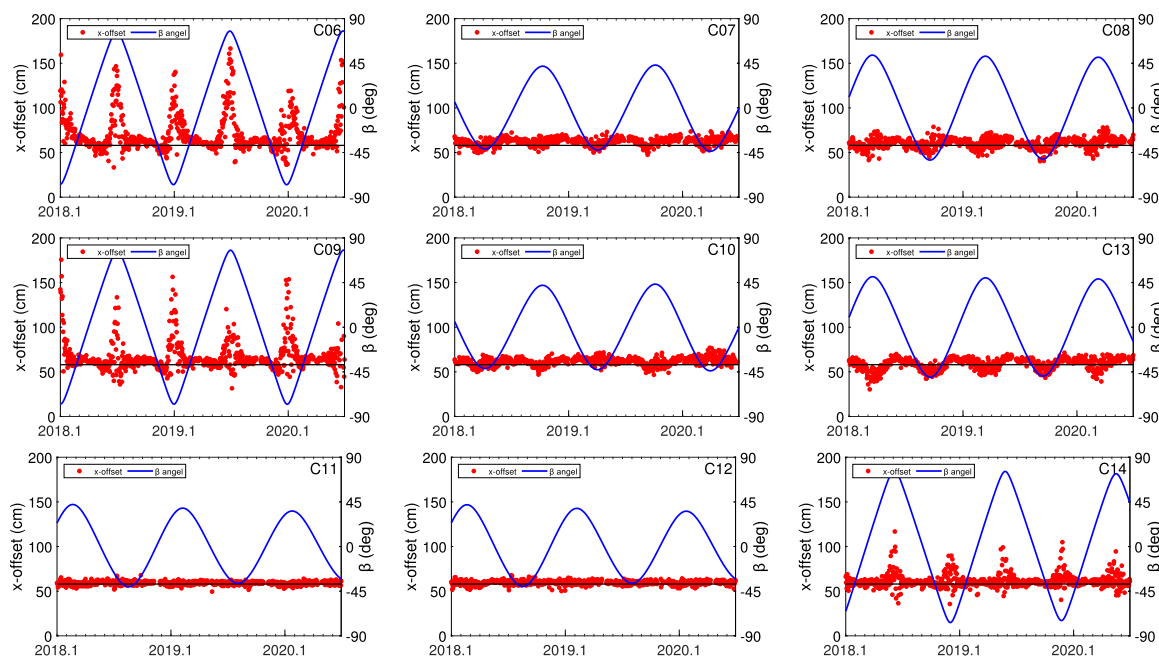
FIGURE 5. Daily estimated x-offset time series for BDS-2 IGSOs (C06, C07, C08, C09, C10 and C13) and MEOs (C11, C12 and C14). The red points are the daily solutions of x-offset, the blue line is the β angle, and the black line is the MGEX value (580.00 mm) of x-offset for comparison.

(Extending the CODE(Center for Orbit Determination in Europe) Orbit Model) as the two vectors almost stay parallel with each other in the inertial frame when orbit-normal mode is adopted. It might cause unexpected PCO values during the deep eclipse periods. That is why the previous PCO time series exclude these parts [22]. In order to achieve a stable solution in the eclipse season, proper constraints should be applied in the orbit-normal phases. Since the mean y-offset only using data out of the orbit-normal periods are close to zero, it is reasonable to tightly constrain y-offset to the initial value during orbit-normal phases. As can be seen from the upper triangle section in Fig.4, the correlation coefficient between y-offset and Y_0 finally turns to a normal level after tight constraint up to 1.0 cm is adopted for y-offsets during the deep eclipse seasons.

B. HORIZONTAL DAILY ESTIMATED PCO TIME SERIES

As for the daily estimated PCO time series, quality control is carried out in advance to detect and get rid of potential outliers. Besides obvious abnormal values with large formal errors are excluded, the rest of horizontal PCO time series are traversed to find any value beyond three-sigma of dynamic average [38]. In this step, less than 1.0% daily estimated PCOs are eliminated for both IGSOs and MEOs, for example, totally six outliers for C07 x-offsets and five for C12 y-offsets are found. After that, the daily estimated horizontal PCO time series of IGSOs and MEOs are plotted in Fig.5 and Fig.6. It should be noted that the vertical-axis on the left is the estimated PCO values, and the vertical-axis on the right is the

corresponding elevation angle β of the Sun above the orbital plane, for the purpose of exploration.

It can be seen from Fig. 5 that the β-dependent systematic effects are more pronounced with peak amplitudes of almost 175.0 cm for C06, C09 and C14, since their particular orbital planes experience a wider range of β angles, for example, $-76.9°$ to $77.0°$ for C06, -77.0 to 77.2 for C09 and -78.2 to 78.1 for C14. While other satellites suffer from less systematic effects because the maximum value of $|\beta|$ is smaller. This indicates a high correlation between the x-offsets and the orbital elements, specifically, the horizontal PCOs are correlated to the along-track orbits when $|\beta|$ is getting larger.

Theoretically, systematic effects in the eclipse season will happen because the solar panels cannot be properly oriented toward the Sun during the eclipse periods. Since a specific strategy of constraining x-offsets to the initial value during orbit-normal phases is adopted. When the absolute value of β angle reaches to zero, the estimated x-offsets are close to the prior value of 580.00 mm. And the corresponding formal errors of x-offsets are less than 1.0 cm due to the residuals between estimated values and initial values are small. Since the low formal errors during these periods, the corresponding x-offsets are included for obtaining the final comprehensive value.

Additionally, seasonal signals with small amplitudes are also detected in the x-offset time series. Theoretically, the annual periodic characteristics are caused by the periodic terms of the right ascension and declination of the Sun. According to [29], the precession of the ascending node $\dot{\Omega}$ of a BDS-2 IGSO and MEO can be calculated as $-2.8°$/year
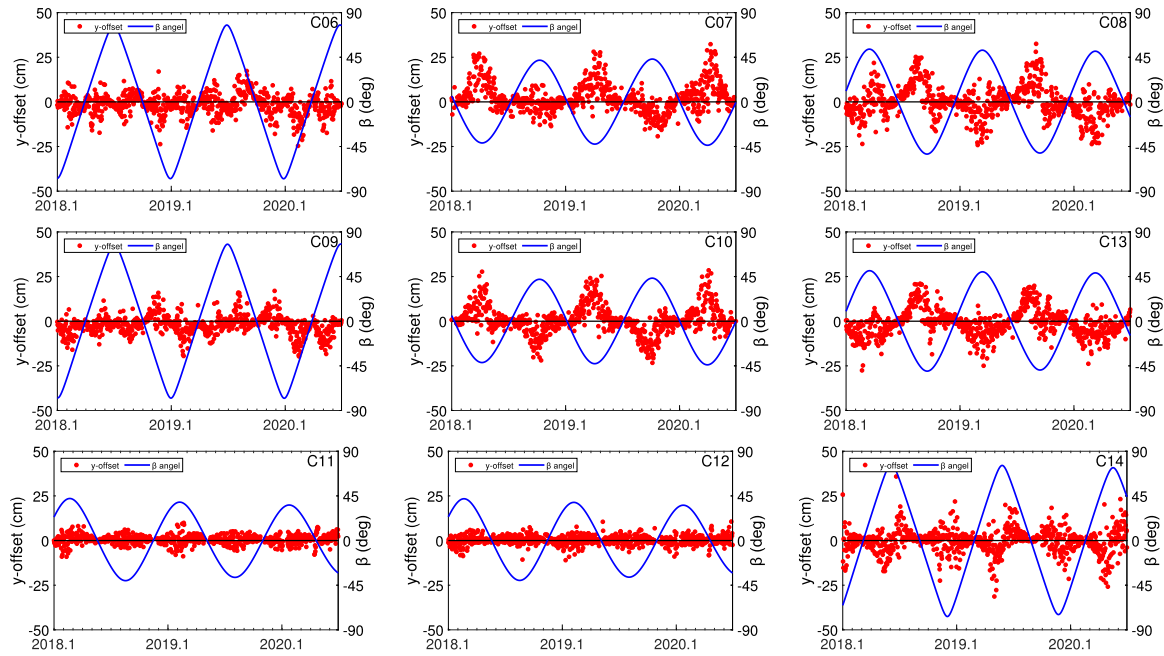
FIGURE 6. Daily estimated y-offset time series for BDS-2 IGSOs (C06, C07, C08, C09, C10 and C13) and MEOs (C11, C12 and C14). The red points are the daily solutions of y-offset, the blue line is the β angle, and the black line is the MGEX value (0.00 mm) of y-offset for comparison. It should be noted that the scale of y-axis is different with that of x-offsets.

and $-11.9°/year$ respectively, using Equation (5).

$$\dot{\Omega} = -3\pi \frac{J_2}{T} \left(\frac{R_e}{a} \right)^2 \cos i \qquad (5)$$

with the orbital period T, the semi-major axis a, the inclination i, the radius of the Earth R_e and the oblateness J_2.

Further, the periods T_R of the signals in Fig. 5 are related to the orientation of the orbital plane with respect to the Sun, and can be calculated as follows,

$$T_R^{IGSO} = \frac{2\pi \cdot 365.25 days}{2\pi - \dot{\Omega}_{IGSO} \cdot 1 year} \approx 362.42 days \qquad (6)$$

$$T_R^{MEO} = \frac{2\pi \cdot 365.25 days}{2\pi - \dot{\Omega}_{MEO} \cdot 1 year} \approx 353.53 days \qquad (7)$$

Meanwhile, spectrum analysis also shows that the main periods of x-offsets are equal to T_R, which are little shorter than one year, and their integer fractions T_R/n, $n = 2, 4, 6, \ldots$ are clearly visible in the spectra of x-offsets. However, the influence of these periodic effects can be reduced or removed by taking an average over a multi-year time interval.

The daily estimated y-offset time series are presented in Fig.6 with the same time span as x-offsets. The β-dependent systematic effects and the seasonal variations are still obvious for IGSOs and MEOs. The peak amplitudes of up to ± 25.0 cm appear during periods with the largest absolute values of β, because the angle between the along track direction and the satellite y-axis closes to 0° or 180° in these cases. It is noted that the maximum amplitude of y-offsets is one-fourth to that of x-offsets in the large $|\beta|$ period. During the deep

eclipse seasons, the satellite starts to rotate around the z-axis with a certain rate [3]. The mismodelling of the yaw angle due to the limited rotation rate will result in the misestimation of y-offset. However, the influence is slight on the daily estimated y-offset since a dominating constraint of up to 1.0 cm is applied on the y-offsets. Therefore, the y-offsets during the eclipse periods are kept in the final combination. Additionally, the y-offsets show a sinusoidal behavior with a peak-to-peak amplitude of 50.0 cm in the period of one year. Spectrum analysis also indicates that two main periods of y-offsets are one year and half a year with smaller amplitudes with respect to x-offsets.

Since the horizontal daily estimated PCO time series behave β-dependent systematic effects, the formal errors of x-offsets and y-offsets are further investigated in this section. The corresponding formal errors of x-offsets and y-offsets versus the β angle are plotted for IGSOs and MEOs in Fig.7. It can be seen that the horizontal PCO formal errors of both types of satellites strongly depend on the β angle. The formal errors increase with increasing the absolute value of the β angle, because of the tight correlation between PCOs and orbital parameters [3]. The largest formal errors of x-offsets and y-offsets occur at C06, C09 and C14, which are nearly 10.0 cm, since the absolute values of β reach their maximum of 78.5° (orbital inclination of satellite 55° plus obliquity of the ecliptic 23.5°). It is indicated that the accuracies of the horizontal PCO estimations are reasonable only when the β angle is getting small, as the formal errors are small. Meanwhile, when the absolute values of β are less than 60°, the formal errors of x-offsets are smaller than that of y-offsets.
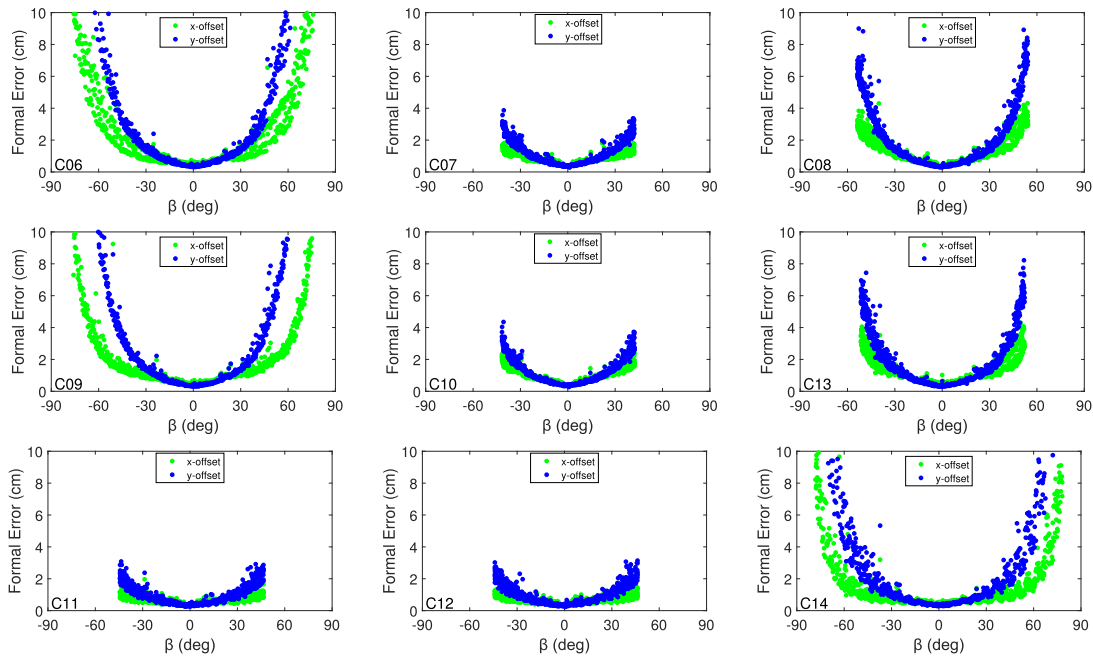
FIGURE 7. The corresponding formal errors of x-offsets and y-offsets versus the β angle for BDS-2 IGSO and MEO satellites.

Similar results were certificated for GPS and Galileo satellites [14].

C. VERTICAL DAILY ESTIMATED PCO TIME SERIES

Many researches indicate that it is possible to estimate PCO corrections when the global terrestrial scale is fixed, because z-offsets are correlated with the global terrestrial scale [3]. Firstly, based on the strategies described in Section III, the average slopes of -25.2 ± 0.9 mm/a in the z-offsets are detected and eliminated. Then, the daily estimated z-offset time series with no evident linear trend for IGSOs and MEOs are plotted in Fig.8.

With the aid of the spectrum analysis, periodic signals can be identified in the z-offset time series. For example, significant annual and sub-annual variations are discovered in some satellites, e.g., C07 and C10. Additionally, it is noted that the maximum range of z-offset in Fig.8 is 500.00 cm, which is much larger than that of horizontal PCOs. It means that the z-offset time series are more scattered compared with horizontal PCOs, but neither show a systematic pattern nor a dependence on the β angle. Nevertheless, the multi-year time series help to limit the impact on the average value [12]. That is why we use a long time series of nearly three years to improve the PCO estimations. As for IGSOs, the estimated z-offsets are varying from satellite to satellite with a low conformity to the MGEX value of 3500.00 mm in igs14_2056.atx, while the estimated z-offsets of MEOs are also smaller than the MGEX value of 2120.00 mm.

D. DERIVATION OF THE COMPREHENSIVE PCOs

The daily PCO time series described in Section IV.B and IV.C are used to generate a set of mean PCOs for BDS-2 satellites

as the final results. It is well known that there are two common methods to derive the mean PCOs. One is the weighted average based on formal errors or the combination of the normal equations. The other is the unweighted average but exclusion of periods with systematic effects based on the β angle or formal errors. It has been proved that the two methods are equivalent and have the same precision [14]. Considering the period of the β angle is one year for BDS-2 satellites, at least two years data are required for the comprehensive solution [25]. Therefore, in order to limit the systematic effects on the average value, nearly three years data are employed to generate the weighted average for the PCO values, based on the corresponding formal errors. Then, the weighted mean PCO for satellite s_i can be calculated as follows,

$$\bar{\mathbf{x}}^{s_i} = \frac{\sum_{j=1}^{n} \mathbf{x}_j^{s_i} \cdot p_j}{\sum_{j=1}^{n} p_j} \quad (8)$$

where $\mathbf{x}_j^{s_i} = \left(x_j^{s_i}, y_j^{s_i}, z_j^{s_i} \right)$ is the jth element in the daily estimated PCO time series for satellite s_i. $p_j = 1 / \sigma_j^2$ is the weight of the jth element in the daily estimated PCO time series, based on the corresponding formal error σ_j. $\bar{\mathbf{x}}^{s_i}$ is the weighted mean PCO for satellite s_i.

The number of used daily estimations and the weighted mean PCO for each satellite are listed in Table 2. The symbol Δ denotes the difference between the weighted mean PCO and the MGEX PCO in the igs14_2056.atx, and its deviation term is the RMS (Root Mean Square) of daily formal
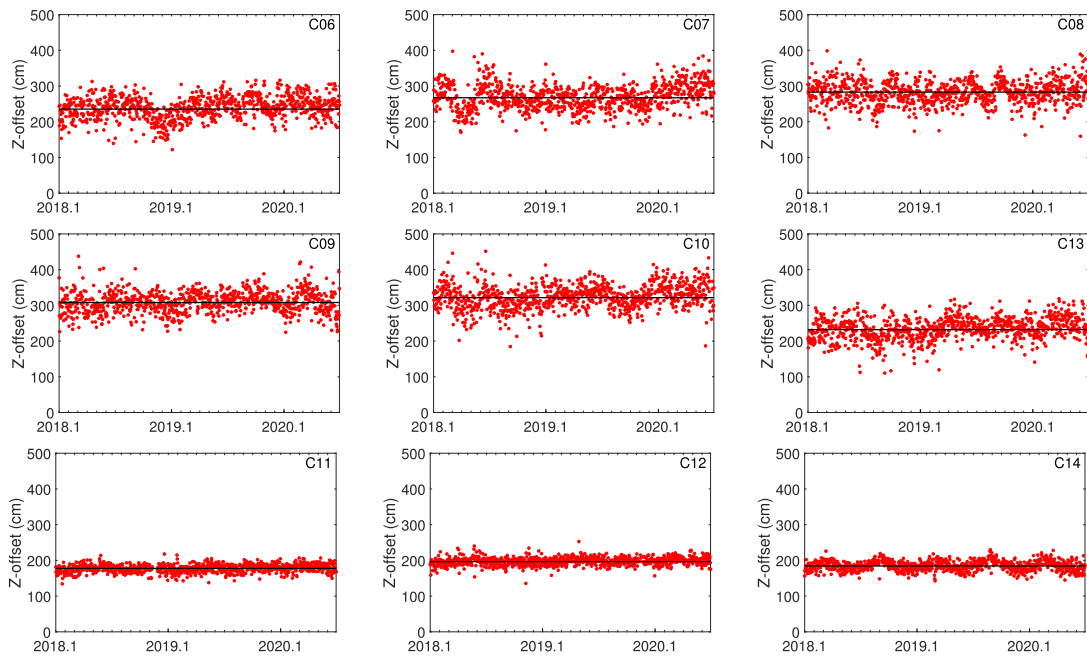
FIGURE 8. Daily estimated z-offset time series for BDS-2 IGSOs (C06, C07, C08, C09, C10, and C13) and MEOs (C11, C12 and C14). The red points are the daily solutions of z-offset, and the black line is the weighted mean value of z-offset. It should be noted that the scale of y-axis is different with that of x-offsets.

TABLE 2. The weighted mean PCOs of BDS-2 satellites with respect to the igs14_2056.atx as the prior information (mm).

Type	PRN	Days	x	y	z	Δx	Δy	Δz
	C06	1295	613.06	0.97	2353.70	33.06±79.22	0.97±0.92	-1146.30±83.21
	C07	1314	626.99	1.20	2671.37	46.99±69.41	1.20±1.30	-828.63±85.43
	C08	1297	613.78	0.06	2829.96	33.78±43.76	0.06±1.52	-670.04±85.84
IGSO	C09	1282	618.58	-2.68	3079.37	38.58±71.34	-2.68±1.34	-420.63±84.13
	C10	1284	621.57	-2.16	3215.12	41.57±50.54	-2.16±1.47	-284.88±91.61
	C13	1303	620.15	-4.77	2320.86	40.15±32.25	-4.77±1.19	-1179.14±91.22
	type-specific		619.02	-0.78	-			
MEO	C11	1268	590.36	6.61	1775.01	10.36±60.21	6.61±1.45	-344.99±33.42
	C12	1280	594.39	2.29	1966.38	14.39±62.86	2.29±1.48	-153.62±34.40
	C14	1300	593.90	2.95	1844.66	13.90±78.55	2.95±1.06	-275.34±34.43
	type-specific		592.88	3.95	-			

errors which indicates the accuracies of the daily estimated PCOs. As shown in Table 2, the weighted mean x-offsets are obtained for IGSOs and MEOs with discrepancies on the level of 4.7 cm and 1.8 cm. Since the PCO values of the same satellite type are similar on the x component, the type-specific comprehensive x-offsets seem to be reasonable. Hence, the weighted mean x-offsets are 619.02 mm for IGSOs and 592.88 mm for MEOs, which are slightly greater than the corresponding values in igs14_2056.atx (580.00 mm). Since the y-offsets are close to zero for all satellites, all the daily estimations including eclipse seasons are applied to derive the weighted average value, and the type-specific mean values of −0.78 mm for IGSOs and 3.95 mm for MEOs are obtained.

If the type-specific z-offset for IGSO satellite is derived, a weighted mean value of 2745.06 mm is obtained

(3500.00 mm in MGEX). However, the differences between each satellite value and the weighted mean value are from −424.20 mm (C13) to 470.06 mm (C10). The peak-to-peak difference is quite considerable, so it is advisable to employ satellite-specific z-offset rather than type-specific value. Similarly, satellite-specific z-offsets for MEOs are more reasonable since the low coherence of these satellites with the same type. Compared with horizontal offsets, z-offsets have a large amount of scatter for both IGSOs and MEOs, and the RMSs for IGSOs are on the 8.7 cm level, which are almost by the factor of two or three with those of MEOs. This is because the higher orbit altitude of the IGSO satellite results in a smaller range of nadir angle, which in turn makes it more difficult to separate the PCOs from other parameters, e.g. clock offsets. Overall, based on these analyses, the final PCOs for BDS-2 IGSOs and MEOs are also summarized in Table 2.
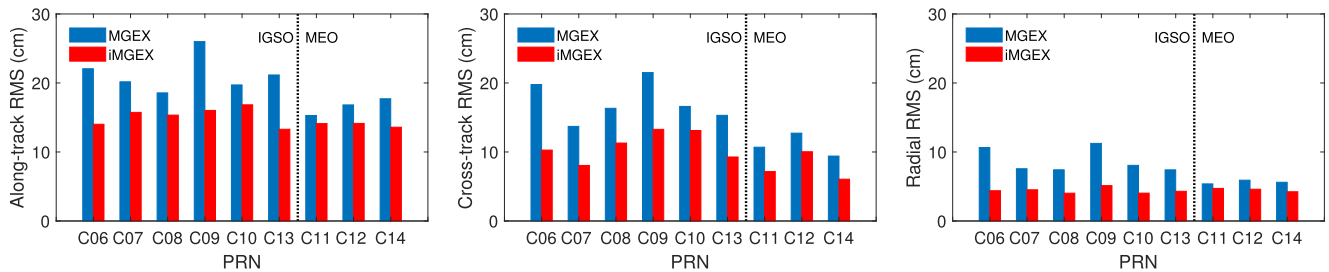
FIGURE 9. The RMSs of the overlapping arcs derived from MGEX and iMGEX PCOs.

V. VALIDATION AND ANALYSIS

In this section, the performances of the improved PCOs are investigated based on the POD and PPP solutions. Firstly, the igs14_2056.atx is compiled for PCOs of BDS-2 satellites. The MGEX PCOs are replaced by the type-specific horizontal PCOs and satellite-specific vertical PCOs listed in Table 2, which generate an updated antenna file called iMGEX for short. In order to validate the performance of iMGEX, the POD and PPP employs the same observations from DOY 090 to 120 in 2018, and the PANDA software is used with the same strategies described in Section III except for the PCOs.

A. PRECISE ORBIT DETERMINATION

1) ORBITAL OVERLAP ANALYSIS

To assess the quality of orbits, orbital overlaps, which represent the orbit consistency, are obtained by 3-day arc POD using MGEX and iMGEX PCOs, respectively. According to orbit overlapping analysis, the orbit of the last day in the first 3-day solution is compared with that of the middle day in the next. The RMSs of the overlapping arcs derived from MGEX and iMGEX values are plotted in Fig. 9.

Compared with the orbits derived from MGEX PCOs, it can be seen from Fig. 9 that the orbit accuracies of IGSOs are improved when considering the newly estimated PCOs. In the along-track component, the mean RMS of IGSOs using updated PCOs is about 15.0 cm, while it is more than 20.0 cm using MGEX PCOs. The improvement for all IGSOs in the along-track component is at rate of 28.5% on average, of which the largest one is 38.3% for C09. The percentage range of improvement in the cross-track component is from 21.0% to 47.9% and the mean value is 36.7%. As for the radial component, two of IGSO satellites benefit obviously from the new PCO estimations, in particular for C06 of 58.8% and C09 of 54.4%, while the other four satellites are improved with more than 40.0%. Overall, it is noticed that IGSOs obtain remarkable benefits from the iMGEX PCOs, although they suffer eclipse during the experimental periods.

Based on the iMGEX PCOs, a better orbit quality is also achieved for MEOs, the average RMSs of orbital overlap differences in the cross-track and radial components are below 10.0 cm and 5.0 cm, while the RMSs in the along-track component show a little worse than 15.0 cm. The orbit accuracies

of three MEO satellites get benefits from the improved PCOs, particularly in the cross-track component, the improvement is of more than 29.2%. As for the along-track and radial components, the improvements are of similar level of 16.0% and 19.8%, respectively. Overall, the internal orbit accuracy revealed by the orbit overlapping analysis show an improvement with average of over 26.3% for both BDS-2 IGSO and MEO satellites when the new estimated PCOs are adopted.

2) SATELLITE LASER RANGING (SLR)

SLR is an independent technique providing external validation for satellite orbits. The laser retroreflector arrays (LRA) are equipped on the BDS-2 satellites to enable SLR tracking by ILRS (International Laser Ranging Service). The SLR residuals are calculated by the differences between the orbits derived from BDS-2 microwave observations and surveyed by the laser trackers, which provides the accuracy assessment mainly for the radial component [39].

SLR tracking station coordinates are fixed to SLRF2014 and the station displacement models are consistent with the IERS (International Earth Rotation Service) conventions, e.g., ocean tidal loading, solid earth tides and the mean pole definition [17]. Due to the data limits, hereby, three satellites, including one MEO satellite C11, two IGSO satellites C08 and C10 for DOY 090 to 120 in 2018 are considered. The SLR residuals of orbits derived from MGEX and iMGEX PCOs for station 7090 (YARL) are shown in Fig.10 as an example. The red points denote the SLR residuals by the iMGEX model, and they are much closer to the black dash of 0.0 cm. Overall, the RMSs are decreased by 52.1%, 33.8% and 35.6% for C08, C10 and C11 respectively, when the improved PCOs are employed.

B. PRECISE POINT POSITIONING

To further assess the qualities of PCO solutions, static PPP has been performed to obtain the global distributed stations coordinates. The validation data of the experimental stations are obtained from Crustal Dynamics Data Information System (CDDIS) servers from DOY 090 to 120 in 2018. And the PCO solutions are derived by the MGEX and iMGEX methods. Then, the RMSs of the stations coordinates are obtained statistically as shown in Fig. 11.
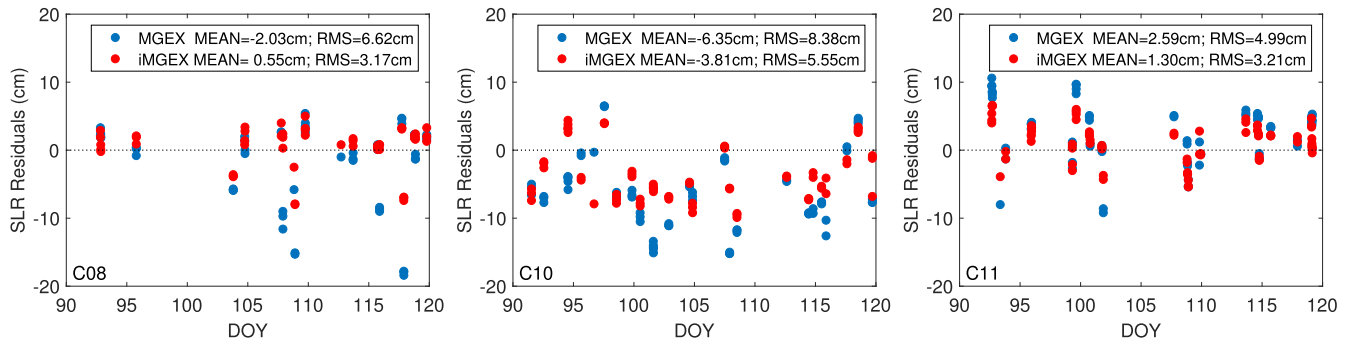
FIGURE 10. The SLR residuals at station 7090 (YARL) for C08, C10 and C11, respectively. The red and blue points denote the SLR residuals obtained by the MGEX and iMGEX PCOs.
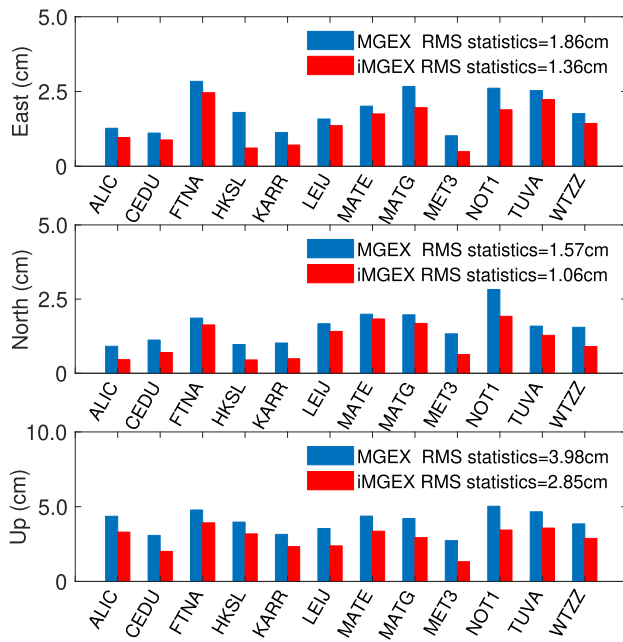

FIGURE 11. The RMSs of the experimental station coordinates between the MGEX and iMGEX PCOs in the east, north and up components, respectively.

When the iMGEX PCOs are employed, Fig.11 shows that the positioning accuracies of the experimental stations are further enhanced. Improvements achieved by the iMGEX method in the east component are at the rate of 27.1% on average. The RMSs discrepancies between the two methods are a little bit large, in particular for the north component, in which the best one is HKSL with the rate of 53.6%. It should be noticed that more than a half stations achieve sub-centimeter accuracies by iMGEX on the north component, while the number is only two by MGEX. It also can be seen that the RMSs of the stations coordinates have significantly decreased on the up component with the minimum of 0.8 cm for FTNA and the maximum of 1.6 cm for NOT1. And the average improvement on the up component for these stations is 1.1 cm. Overall, iMGEX achieves a further improvement of 27.1%, 32.6% and 28.4% compared with MGEX on the east, north, and up component.

VI. SUMMARY AND CONCLUSION

The satellite PCO is the offset between the CoM and antenna phase center, and plays a key role in the precise orbit determination and positioning. Even if the satellite PCO can be calibrated before launch, however, the value changes with operational status of each satellite and the complex space environments. Firstly, the satellite PCO is related to the attitude model, so the PCO value should be reestimated when a new attitude model is established. Meanwhile, the CoM of a satellite also changes because of the fuel consumption and component aging. Hence, the PCO of a satellite has to be determined and updated continuously. As a newly built constellation, establishing more sophisticated models for BDS-2 satellites is a promising approach to enhance their solutions, in particular for the PCO values. In order to improve the quality of precise applications, this paper focuses on improved satellite PCOs for BDS-2 IGSOs and MEOs, in which GEOs are excluded due to the weak ground station observation geometry.

After a careful investigation for the constraints on the satellite PCOs during orbit-normal phases, the daily estimated PCOs are obtained using nearly three years MGEX observations, and the systematic effects depending on the elevation angle of the Sun with respect to the orbital plane and seasonal variations are explored. The horizontal PCO time series and the corresponding formal errors are sensitive to the β angle which are caused by high correlations between the orbital parameters and PCOs. The effects to x-offsets are more pronounced than y-offsets, in particular for C06, C09 and C14, which experience a larger elevation angle range. The eclipse has little influence on x-offsets and y-offsets when suitable constraints are employed. On the contrary, no evident β-dependent systematic effects are found in z-offset time series and their formal errors. However, the difference of z-offsets between each satellite is quite large up to more than 1.4 m at maximum, and it is advisable to employ satellite-specific z-offsets rather than type-specific values. Therefore, the final PCO results are given in Table 2 with type-specific horizontal offsets and satellite-specific vertical offsets by the weighted mean method using formal errors as the weights.

Furthermore, for the purpose of validation and analysis, the performances of the improved PCOs are investigated

based on the POD and PPP solutions, and the satellite orbits and station coordinates are obtained and compared using the original MGEX PCOs and the improved PCOs, respectively. Firstly, orbital overlap analysis is performed, and the internal orbit accuracies show an improvement with average of over 26.3% for both BDS-2 IGSO and MEO satellites when the improved PCOs are adopted. Meanwhile, the SLR residuals of orbits derived from MGEX and iMGEX values illustrate the improvements on the radial component for C08, C10 and C11 are around 40.5% on average. For the static PPP, iMGEX achieves improvements of 27.1%, 32.6% and 28.4% on the east, north, and up component respectively, compared with MGEX, and more than a half experimental stations achieve sub-centimeter positioning accuracy by iMGEX on the north component.
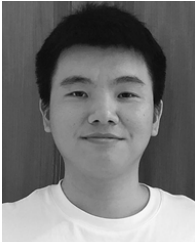
REFERENCES

[1] M. Ge, H. Zhang, X. Jia, S. Song, and J. Wickert, "What is achievable with the current COMPASS constellations," in *Proc. 25th Int. Tech. Meeting Satell. Division Inst. Navigat. (ION GNSS)*, Nashville, TN, USA, Sep. 2012, pp. 17–21.

[2] C. Shi, Q. Zhao, M. Li, W. Tang, Z. Hu, Y. Lou, H. Zhang, X. Niu, and J. Liu, "Precise orbit determination of beidou satellites with precise positioning," *Sci. China Earth Sci.*, vol. 55, no. 7, pp. 1079–1086, Jul. 2012.

[3] R. Schmid, P. Steigenberger, G. Gendt, M. Ge, and M. Rothacher, "Generation of a consistent absolute phase-center correction model for GPS receiver and satellite antennas," *J. Geodesy*, vol. 81, no. 12, pp. 781–798, Nov. 2007.

[4] R. Dach, R. Schmid, M. Schmitz, D. Thaller, S. Schaer, S. Lutz, P. Steigenberger, G. Wübbena, and G. Beutler, "Improved antenna phase center models for GLONASS," *GPS Solutions*, vol. 15, no. 1, pp. 49–65, Jan. 2011.

[5] S. Y. Zhu, F.-H. Massmann, Y. Yu, and C. Reigber, "Satellite antenna phase center offsets and scale errors in GPS solutions," *J. Geodesy*, vol. 76, nos. 11–12, pp. 668–672, Mar. 2003.

[6] O. Montenbruck, A. Hauschild, P. Steigenberger, U. Hugentobler, P. Teunissen, and S. Nakamura, "Initial assessment of the COMPASS/BeiDou-2 regional navigation satellite system," *GPS Solutions*, vol. 17, no. 2, pp. 211–222, Apr. 2013.

[7] M. Li, L. Qu, Q. Zhao, J. Guo, X. Su, and X. Li, "Precise point positioning with the BeiDou navigation satellite system," *Sensors*, vol. 14, no. 1, pp. 927–943, Jan. 2014.

[8] G. L. Mader and F. Czopek, "Calibrating the L1 and L2 phase centers of a block IIA antenna," in *Proc. 14th Int. Tech. Meeting Satell. Division Inst. Navigat. (ION GPS)*, Salt Lake City, UT, USA, Sep. 2001, pp. 1979–1984.

[9] R. Schmid and M. Rothacher, "Estimation of elevation-dependent satellite antenna phase center variations of GPS satellites," *J. Geodesy*, vol. 77, nos. 7–8, pp. 440–446, Oct. 2003.

[10] R. Schmid, M. Rothacher, D. Thaller, and P. Steigenberger, "Absolute phase center corrections of satellite and receiver antennas: Impact on global GPS solutions and estimation of azimuthal phase center variations of the satellite antenna," *GPS Solutions*, vol. 9, no. 4, pp. 283–293, Nov. 2005.

[11] M. Ge and G. Gendt, "Estimation of IGS absolute antenna phase center variations," in *Proc. IGS Workshop Symp.*, M. Meindl, Ed. Bern, Switzerland, 2005, pp. 1–7.

[12] R. Schmid, R. Dach, X. Collilieux, A. Jäggi, M. Schmitz, and F. Dilssner, "Absolute IGS antenna phase center model igs08.atx: Status and potential improvements," *J. Geodesy*, vol. 90, no. 4, pp. 343–364, Apr. 2016.

[13] F. Dilssner, T. Springer, C. Flohrer, and J. Dow, "Estimation of phase center corrections for GLONASS-M satellite antennas," *J. Geodesy*, vol. 84, no. 8, pp. 467–480, Aug. 2010.

[14] P. Steigenberger, M. Fritsche, R. Dach, R. Schmid, O. Montenbruck, M. Uhlemann, and L. Prange, "Estimation of satellite antenna phase center offsets for galileo," *J. Geodesy*, vol. 90, no. 8, pp. 773–785, Aug. 2016.

[15] J. Guo, X. Xu, Q. Zhao, and J. Liu, "Precise orbit determination for quad-constellation satellites at Wuhan University: Strategy, result validation, and comparison," *J. Geodesy*, vol. 90, no. 2, pp. 143–159, Feb. 2016.

[16] X. Li, Y. Zhu, K. Zheng, Y. Yuan, G. Liu, and Y. Xiong, "Precise orbit and clock products of galileo, BDS and QZSS from MGEX since 2018: Comparison and PPP validation," *Remote Sens.*, vol. 12, no. 9, p. 1415, Apr. 2020.

[17] O. Montenbruck, P. Steigenberger, L. Prange, Z. Deng, Q. Zhao, F. Perosanz, I. Romero, C. Noll, A. Stürze, G. Weber, R. Schmid, K. MacLeod, and S. Schaer, "The multi-GNSS experiment (MGEX) of the international GNSS service (IGS)—Achievements, prospects and challenges," *Adv. Space Res.*, vol. 59, no. 7, pp. 1671–1697, Apr. 2017.

[18] *IGS MAIL-7126.* Accessed: Jul. 31, 2015. [Online]. Available: http://lists.igs.org/pipermail/igsmail/2015/000960.html

[19] Y. Lou, Y. Liu, C. Shi, X. Yao, and F. Zheng, "Precise orbit determination of BeiDou constellation based on BETS and MGEX network," *Sci. Rep.*, vol. 4, no. 1, May 2015, Art. no. 4692.

[20] J. Guo, "The impacts of attitude, solar radiation and function model on precise orbit determination for GNSS satellites," Ph.D. dissertation, GNSS Res. Center, Wuhan Univ., Wuhan, China, 2014.

[21] F. Dilssner, T. Springer, and E. Enderle, "Estimation of satellite antenna phase center corrections for BeiDou," in *Proc. IGS Workshop*, Pasadena, CA, USA, Jun. 2014, pp. 23–27.

[22] G. Huang, X. Yan, Q. Zhang, C. Liu, L. Wang, and Z. Qin, "Estimation of antenna phase center offset for BDS IGSO and MEO satellites," *GPS Solutions*, vol. 22, no. 2, p. 49, Apr. 2018.

[23] O. Montenbruck, P. Steigenberger, and A. Hauschild, "Broadcast versus precise ephemerides: A multi-GNSS perspective," *GPS Solutions*, vol. 19, no. 2, pp. 321–333, Apr. 2015.

[24] *IGS ATX Products.* Accessed: Jun. 29, 2019. [Online]. Available: https://igs.org/pub/station/general/pcv_archive/igs14_2056.atx

[25] X. Yan, G. Huang, Q. Zhang, L. Wang, Z. Qin, and S. Xie, "Estimation of the antenna phase center correction model for the BeiDou-3 MEO satellites," *Remote Sens.*, vol. 11, no. 23, p. 2850, Nov. 2019.

[26] C. Wang, J. Guo, Q. Zhao, and J. Liu, "Yaw attitude modeling for BeiDou I06 and BeiDou-3 satellites," *GPS Solutions*, vol. 22, no. 4, Oct. 2018, Art. no. 117.

[27] L. He, M. Ge, J. Wang, J. Wickert, and H. Schuh, "Experimental study on the precise orbit determination of the BeiDou navigation satellite system," *Sensors*, vol. 13, no. 3, pp. 2911–2928, Mar. 2013.

[28] O. Montenbruck, R. Schmid, F. Mercier, P. Steigenberger, C. Noll, R. Fatkulin, S. Kogure, and A. S. Ganeshan, "GNSS satellite geometry and attitude models," *Adv. Space Res.*, vol. 56, no. 6, pp. 1015–1029, Sep. 2015.

[29] O. Montenbruck and E. Gill, *Satellite Orbits: Models, Methods and Applications*, 2nd ed. Berlin, Germany: Springer, 2000.

[30] P. Steigenberger, U. Hugentobler, A. Hauschild, and O. Montenbruck, "Orbit and clock analysis of compass GEO and IGSO satellites," *J. Geodesy*, vol. 87, no. 6, pp. 515–525, Jun. 2013.

[31] S. Ye, L. Zhao, J. Song, D. Chen, and W. Jiang, "Analysis of estimated satellite clock biases and their effects on precise point positioning," *GPS Solutions*, vol. 22, no. 1, p. 16, Jan. 2018.

[32] P. Li, X. Zhang, M. Ge, and H. Schuh, "Three-frequency BDS precise point positioning ambiguity resolution based on raw observables," *J. Geodesy*, vol. 92, no. 12, pp. 1357–1369, Dec. 2018.

[33] M. Ge, G. Gendt, M. Rothacher, C. Shi, and J. Liu, "Resolution of GPS carrier-phase ambiguities in precise point positioning (PPP) with daily observations," *J. Geodesy*, vol. 82, no. 7, pp. 389–399, Jul. 2008.

[34] T. A. Springer, G. Beutler, and M. Rothacher, "Improving the orbit estimates of GPS satellites," *J. Geodesy*, vol. 73, no. 3, pp. 147–157, Apr. 1999.

[35] J. Boehm, B. Werl, and H. Schuh, "Troposphere mapping functions for GPS and very long baseline interferometry from European centre for medium-range weather forecasts operational analysis data," *J. Geophys. Res., Solid Earth*, vol. 111, no. B2, pp. 1–9, Feb. 2006.

[36] J. Saastamoinen, "Contributions to the theory of atmospheric refraction," *Bull. géodésique*, vol. 105, no. 1, pp. 279–298, Sep. 1972.

[37] F. Xia, S. Ye, D. Chen, and N. Jiang, "Observation of BDS-2 IGSO/MEOs yaw-attitude behavior during eclipse seasons," *GPS Solutions*, vol. 23, no. 3, Jul. 2019.

[38] C. Ghilani, "Adjustment computations: Spatial data analysis," in *Random Error Theory*, 6th ed. Toronto, ON, Canada: Wiley, 2017, p. 50.

[39] K. Sośnica, L. Prange, K. Kaźmierski, G. Bury, M. Drożdżewski, R. Zajdel, and T. Hadas, "Validation of galileo orbits using SLR with a focus on satellites launched into incorrect orbital planes," *J. Geodesy*, vol. 92, no. 2, pp. 131–148, Feb. 2018.

LINA HE received the B.S. degree in surveying and mapping engineering from Hohai University, Nanjing, China, in 2007, and the M.S. and Ph.D. degrees in geodesy from Tongji University, Shanghai, China, in 2010 and 2013, respectively. She is currently an Associate Professor with the School of Earth Sciences and Engineering, Hohai University. Her research interests include satellite orbit determination and data processing for global navigation satellite systems (GNSSs).

PING ZENG received the B.S. degree in surveying and mapping engineering from the Institute of Disaster Prevention, Langfang, China, in 2019. He is currently pursuing the M.S. degree in geodesy with the School of Earth Sciences and Engineering, Hohai University. His research interests include GNSS precise point positioning (PPP) and data processing.

HAIRUI ZHOU (Member, IEEE) received the B.S. and Ph.D. degrees in control theory and engineering from Northwestern Polytechnical University, Xi'an, China, in 2004 and 2010, respectively. His research interests include positioning, navigation and timing, high-speed networks, and wireless sensor networks.

YUANLAN WEN received the B.S. and M.S. degrees from the Zhengzhou Institute of Surveying and Mapping, Zhengzhou, China, in 1988 and 1993, respectively, and the Ph.D. degree from Information Engineering University, Zhengzhou, in 2001. He is currently a Professor with the School of Earth Sciences and Engineering, Hohai University. His research interests include GNSS data processing and precise orbit determination.

• • •